$$D_l = 2\int_{x_h}^{1} \mathrm{d}x D_0(x) \tag{39}$$

Substituting the representations of $P_{1,2}$ from Eq. (18), we find, after some manipulation, that

$$D_m(x_h) = \sum_{i=0}^{n-1} \sum_{j=i+1}^{n} \mathrm{d}_{ij} E_{ij}^{(m)}(x_h) \tag{40}$$

where

$$\mathrm{d}_{ij} = a_{2i}a_{1j} - a_{2j}a_{1i} \tag{41}$$

The E are elementary functions, if rather elaborate ones. They are most compactly expressible in terms of the V_j [Eq. (30)] and the related functions

$$U_j(x_{hj}) = \begin{cases} \frac{1}{2}(\cos^{-1}x_h)^2 & (j=0) \\ 1/j^2(1-\cos(j\cos^{-1}x_h) & (j\neq 0) \end{cases} \tag{42}$$

$$\hat{U}_j = jU_j \tag{43}$$

$i+j$ odd

$$E_{ij}^{(0)} = (-1)^i V_i V_j \tag{44}$$

$$E_{ij}^{(1)} = \begin{cases} \dfrac{(-1)^i}{2ij}(\hat{U}_{j-i+1} - \hat{U}_{j-i-1} + \hat{U}_{j+i-1} - \hat{U}_{j+i+1} & (i\neq 0) \\ \dfrac{1}{j}(V_0(V_{j-1} - V_{j+1}) + U_{j+1} - U_{j-1}) & (i=0) \end{cases} \tag{45}$$

$i+j$ even

$$E_{ij}^{(0)} = \begin{cases} (-1)^i \dfrac{i^2-j^2}{2ij}(U_{i+j} - U_{j-i}) & (i\neq 0) \\ 2U_j - V_0 V_j & (i=0) \end{cases} \tag{46}$$

$$E_{ij}^{(1)} = \begin{cases} 2(U_1-1)E_{ij}^{(0)} \\ \quad + \dfrac{(-1)^i}{2ij}[(i-j)(\hat{U}_{i+j+1} + \hat{U}_{i+j-1}) \\ \quad + (i+j)(\hat{U}_{j-i+1} + \hat{U}_{j-i-1})] & (i\neq 0) \\ 4U_1/j^2 + \dfrac{1}{J^2}[(3j-2)U_{j-1} - (3j+2)U_{j+1}] \\ \quad - \dfrac{1}{j}V_0(V_{j-1} - V_{j+1}) & (i=0) \end{cases} \tag{47}$$

Conclusions

Simple universal formulas have been given for the most important aerodynamic coefficients in unsteady thin airfoil theory. The lift and moment induced by a generalized gust are evaluated explicitly in terms of the gust wavelength. Similarly, in the control surface problem, the lift, moment, and hinge moments are given as explicit algebraic functions of hinge location. These results can be used in conjunction with any of the standard numerical inversion routines for the elementary loads (pitch and heave).

Acknowledgement

This work was suppoted by NASA Grant NSG 2194.

References

[1] Williams, M. H., "Exact Solutions in Oscillating Airfoil Theory," *AIAA Journal*, Vol. 15, June 1977, p. 875.

[2] Kemp, N. H., "Simplified Formulas for Lift and Moment in Unsteady Thin Airfoil Theory," *AIAA Journal*, Vol. 16, Aug. 1978, p. 851.

[3] Williams, M. H., "The Inversion of Singular Integral Equations by Expansion in Jacobi Polynomials," *Journal of the Institute of Mathematics and Its Applications*, to be published.

[4] Sears, W. R., ed., "Reciprocity Relations and Reverse Flow Theorems in Aerodynamics," *General Theory of High Speed Aerodynamics*, Vol. 6, Princeton University Press, Princeton, N.J., 1954, pp. 314-327.

J80-161

Separation Pressure of a Turbulent Boundary Layer in Transonic Interactions

20003
20007
20018

A. G. Panaras*
Von Kármán Institute for Fluid Dynamics, Belgium

Introduction

A SEMIEMPIRICAL method for the calculation of the downstream characteristics of a boundary layer interacting with a shock is called "discontinuity analysis." The basis of this method is the omission of the shear stress term from the x-momentum equation as being negligible compared with the pressure gradient term, and the derivation of equations which give the overall development of some critical characteristics of the boundary layer under the impact of a given pressure jump Δp, the strength of the shock. In this kind of analysis no length scale appears and, apart from the convenience of ignoring the length of the interaction, which is an unknown quantity, this independence from length scales simplifies the equations and provides similarity relations which efficiently describe the physical mechanisms controlling the overall development of the boundary layer.

The most widely known discontinuity analysis is the one of Reshotko and Tucker,[1] while Green[2] has classified the various approaches which are based on this principle and justified their use by presenting comparisons with experimental data.

More recently, the present author has developed a new discontinuity analysis[3] in which the similarity relations giving the development of the thickness quantities δ^* and ϑ are made more precise through inclusion of the thickening of the boundary layer itself. As a result, the agreement with the experimental evidence is better than the methods reviewed by Green. An additional difference between our analysis and the method of Reshotko and Tucker is the possibility in the former approach of including mass entrainment, which in the higher transonic numbers is significant, while the latter approach is based strictly on the zero entrainment principle.

Apart from the downstream characteristics of an interacting turbulent boundary layer,[4,5] our analysis provides a new incipient separation criterion and gives an explanation for the observed behavior of the pressure at the separation point, for increasing upstream Mach number, and for varying initial conditions of the boundary layer. In this Note those latter aspects of the interaction problem will be presented.

Received June 25, 1979; revision received Oct. 29, 1979. Copyright © American Institute of Aeronautics and Astronautics, Inc. 1979. All rights reserved.

Index categories: Boundary Layers and Convective Heat Transfer—Turbulent; Jets, Wakes, and Viscid-Inviscid Flow Interactions; Transonic Flow.

*Presently, Head of Aerodynamics Section, HAF Technology Research Center, Palaion Faliron, Athens, Greece. Member AIAA.

Derivation of the Fundamental Equation

The basic equations which we use in the discontinuity analysis are the classical momentum and energy integral equations, after the omission of the viscous terms. Proper combination of those equations provides the following relation, which contains shape factors instead of thickness quantities:

$$\frac{du_e}{u_e} = \frac{1}{H-1-R(\gamma-1)M_e^2}\frac{dH_{32}}{H_{32}} \tag{1}$$

where

$$H=\delta^*/\vartheta, \quad H_{32}=\delta^{**}/\vartheta$$

The right-hand side of Eq. (1) is the differential of the shape parameter L of Truckenbrodt extended to the compressible flow. For the integration, knowledge of the relation $H=f(H_{32},M_e)$ is necessary. This is easily obtained if a compressible velocity profile is used. In Fig. 1, the curves $L=f(M,H_i)$ after Huo[6] are shown for the transonic region of flow. The parameter H_i is the widely known kinetic shape factor. We observe that the value $L=0$ corresponds to separation ($H_i=2.4$).

If a velocity drop from an initial condition "1" to a final condition "2" is considered, it is found that Eq. (1) yields

$$L_2=L_1-\ln u_{e_1}/u_{e_2} \tag{2}$$

This is the fundamental equation for our analysis as it describes how the velocity profile of a boundary layer is deformed under the influence of a sudden pressure increase.

Derivation of an Incipient-Separation Criterion

If the deformation of the velocity profile of the turbulent boundary layer under the impact of the shock-caused pressure jump is such as to cause the shape factor H_{i2} to attain the separation value, we presume that the shock has induced incipient separation. Obviously, the point where the incipient separation occurs lies downstream of the shock, at the end of the interaction zone. Having defined $L_2=0$ at the separation point, for a given upstream Mach number (M_{e_1}) Eq. (2) provides the required initial value L_1 of the shape parameter for the occurrence of incipient separation if the velocity drop is known. Specifically, for the case of a normal shock Eq. (2) is written as

$$L_1=\ln\frac{(\gamma+1)M_{e_1}^2}{(\gamma-1)M_{e_1}^2+2} \tag{3}$$

The influence of the Reynolds numbers does not appear explicitly in Eq. (3) so the calculations of the curve $L_1=f(M_{e_1})$ can be carried out once and for all. Using the shape factor H_{i_1} as an independent variable we have calculated the incipient separation curve for the transonic flow regime. The curve is shown in Fig. 2 together with some experimental points. The agreement of the predicted values with the marked experimental points is good.

The proposed separation criterion implicitly presents all the experimentally observed features. Thus, it is known that for favorable pressure gradients ahead of the shock a stronger shock is required to induce separation, whereas for adverse pressure gradients ahead of the shock a weaker shock would separate the turbulent boundary layer. Moving along the separation line in Fig. 2, however, we observe that the lower the H_{i_1} is (accelerating flows), the higher the Mach number becomes for the occurrence of separation. Similarly, Fig. 2 indicates that a boundary layer subjected to an adverse pressure gradient (increasing values of H_{i_1}) separates at a lower Mach number.

The effect of increasing Reynolds number is to delay separation. This feature is also described in Fig. 2, because increase of Reynolds number means decrease of the shape parameter H_{i_1}.

If the upstream Mach increases, after the establishment of incipient separation the separation bubble grows, the

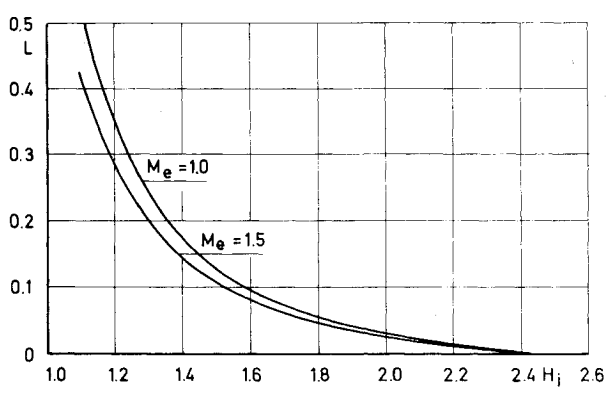

Fig. 1 Shape factor L variation.

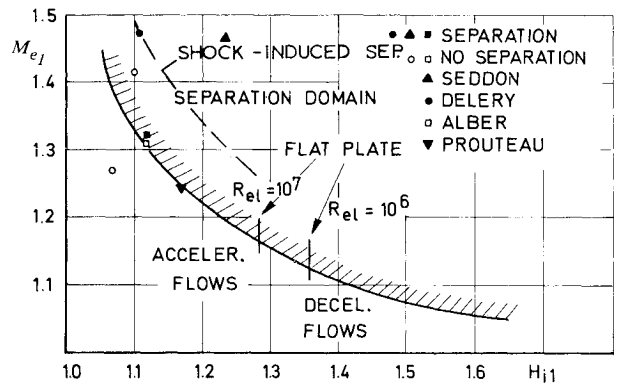

Fig. 2 Separation criterion.

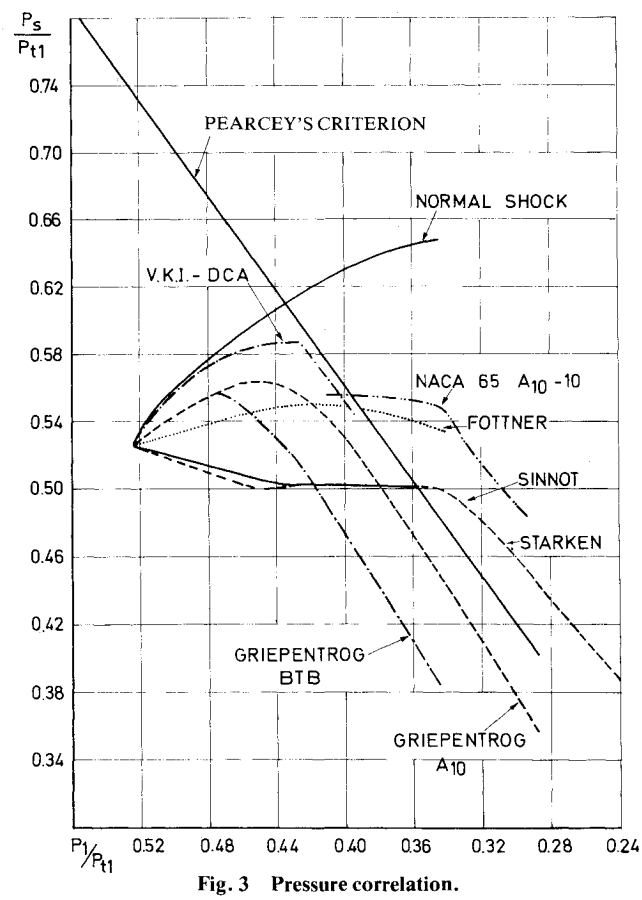

Fig. 3 Pressure correlation.

separation point moves upstream, and finally the lambda shock pattern appears. This state has been named shock-induced separation and it has been assumed that it appears when the separation pressure equals the pressure for sonic conditions.[7] According to the various empirical criteria, this type of separation appears for $M_{e_1} \cong 1.27\text{-}1.33$

If Eq. (2) is solved for $M_{e_2} = 1$, the theoretical criterion of shock-induced separation is obtained. In this case we assume $L_2 = 0.05$. This is the experimental value of the shape factor L for mixed flow separation profile.[3] In Fig. 2 this criterion is shown as a dashed line for the case of accelerated flows. We observe that generally the theoretical calculation verifies the empirical criteria. However, it also indicates that for highly accelerated boundary layers the shock-induced separation may appear for higher Mach numbers than 1.33.

Calculation of the Separation Pressure

Equation (2) will be used in this paragraph for the calculation of the pressure at the separation point. For this, we just have to estimate u_{e_2} (or M_{e_2}) for L_2 corresponding to separation. Furthermore, by representating graphically the relation $M_{e_2} = f(L, M_{e_1})$ it will be possible to explain the observed behavior of the separation pressure.

The experimental behavior of the separation pressure has been summarized by Chauvin,[8] who has made a survey of the existing experimental pressure correlations and has presented them in an illustrative form (Fig. 3). In his analysis Chauvin observes that almost all the data show the same tendency, that is, first a more or less pronounced increase of downstream static pressure with decreasing upstream static pressure (the same tendency as for the normal shock), followed by a more or less abrupt knee, and then by a linear decrease of downstream pressure as the upstream pressure further diminishes, with approximately the same slope as that indicated by Pearcey's criterion. The "knee" and the subsequent linear decrease in downstream pressure ratio have been generally attributed to a local separation bubble which grows with the Mach number upstream of the shock, eventually reaching the trailing edge. No explanation for the lateral spacing of the curves in Fig. 3 has been given.

If Eq. (2) is combined with the oblique-shock velocity relation, the following equation is obtained:

$$\frac{M_{e_2}}{M_{e_1}} = B \Big/ \left(1 + \frac{\gamma - 1}{2} B^2\right)^{1/2} \tag{4}$$

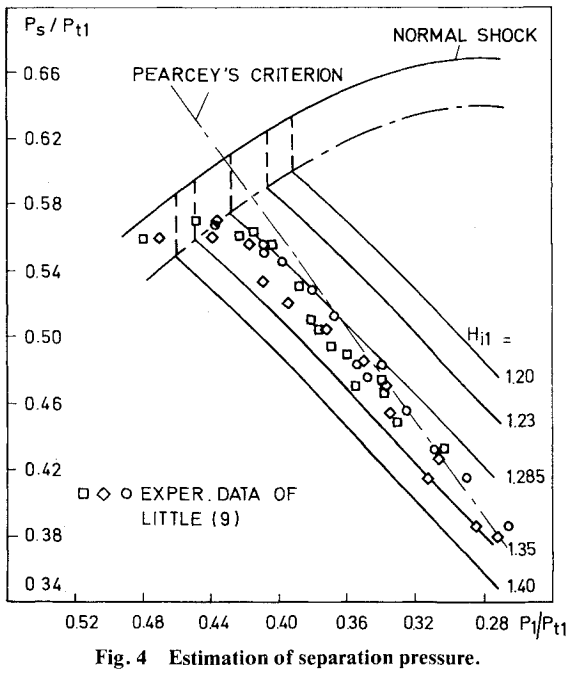

Fig. 4 Estimation of separation pressure.

where

$$B = [\exp(L_2 - L_1)] \Big/ \left(1 + \frac{\gamma - 1}{2} M_{e_1}^2\right)^{1/2} \tag{5}$$

Instead of using the quantity L_1 as a parameter we may replace by the shape factor H_{i_1}. In Fig. 4 we have drawn the curves $p_s/p_{t_1} = f(p_1/p_{t_1}, H_{i_1})$. The calculated curves $H_{i_1} = \text{const.}$ are asymptotically almost parallel straight lines. Additionally, along each of these curves the Mach number ratio M_{e_2}/M_{e_1} remains practically constant.

The presentation of Eq. (4) on the plane (p_1, p_s) shows that the "knee" and the subsequent decrease in the separation pressure are not due to the size of the separation bubble, but to the existence of a similarity law which describes how a velocity profile is transformed into a separating one. According to this law, which has been revealed by the discontinuity analysis approach, the transformation of a velocity profile 1 into another 2 because of the action of pressure forces depends rather on the ratio of the Mach numbers M_{e_1} and M_{e_2} and not on their absolute values. For given constant shapes of the profiles 1 and 2 the ratio M_{e_2}/M_{e_1} retains a constant value if the upstream Mach number M_{e_1} changes.

Variation of the shape 1 or 2 induces variation of the Mach number ratio. Quantitatively, this variation is given by Eq. (4). The dependence of the value of the ratio M_{e_2}/M_{e_1} on the initial shape of the velocity profile justifies the observed lateral spacing of the experimental curves.

In Fig. 4 we have marked the experimental data of Little,[9] which were obtained in an axisymmetric nozzle. The points are ordered in a way qualitatively confirming the validity of the theoretical calculations. Little has performed measurements of the velocity profile and each symbol in the diagram corresponds to a constant upstream profile, hence the observed small scattering of the data. The measurements were performed at the end of the constant area portion of the test nozzle, however, far upstream of the shock. Thus, they do not represent the initial conditions of the boundary layer at the interaction zone and we cannot check for quantitative agreement. However, in Ref. 3, quantitative comparisons with other proper data have been performed. The agreement is rather good.

References

[1] Reshotko, E. and Tucker, M, "Effect of a Discontinuity on Turbulent Boundary Layer Thickness Parameters with Application to Shock-Induced Separation," NACA TN 3454, 1955.

[2] Green, J. E., "Interactions between Shock Waves and Turbulent Boundary Layers," *Progress in Aeronautical Sciences*, Vol. 11, Pergamon, New York, 1970, pp. 235-348.

[3] Panaras, A. G., "Calculation of a Boundary Layer Interacting with a Normal Shock by a Discontinuity Analysis," VKI TN 121, Oct. 1976.

[4] Panaras, A. G. and Inger, G. R., "Transonic Normal Shock-Turbulent Boundary Layer Interaction in Pressure Gradient Flows," ASME Paper No. 77-GT-34, March 1977.

[5] Van Den Braembussche, R., "The Prediction of Compressor Blade Row Performance: Numerical Methods and Theoretical Approaches," VKI LS 1978-2, Feb. 1978.

[6] Huo, S., "Optimization Based on Boundary Layer Concept for Compressible Decelerating Flows," Ph.D. thesis, Univ. Libre de Bruxelles, 1973.

[7] Alber, I. E., Bacon, J. W., Masson, B. S., and Collins, D. J., "An Experimental Investigation of Turbulent Transonic Viscous-Inviscid Interactions," *AIAA Journal*, Vol. 11, May 1973, pp. 620-627.

[8] Chauvin, J., "Shock-Boundary Layer Interaction in Compressor Cascade. A Review of Available Data," VKI LS 59, 1973.

[9] Little, B. H., Jr., "Effects of Initial Turbulent Boundary Layer on Shock-Induced Separation in Transonic Flow," VKI TN 39, 1967.